Proceedings of the Combustion Institute 40 (2024) 105529

Contents lists available at ScienceDirect

Proceedings of the Combustion Institute

journal homepage: www.elsevier.com/locate/proci

The role of chemistry in the retardant effect of dimethyl methylphosphonate in flame–wall interaction

Federica Ferraro [a], Alessandro Stagni [b,*], Arne Scholtissek [c]

[a] Technische Universität Braunschweig, Institute of Jet Propulsion and Turbomachinery, Braunschweig, Germany
[b] Department of Chemistry, Materials, and Chemical Engineering "G. Natta", Politecnico di Milano, Milano 20133, Italy
[c] Technical University of Darmstadt, Department of Mechanical Engineering, Simulation of reactive Thermo-Fluid Systems, Darmstadt, Germany

ARTICLE INFO

Keywords:
Flame–wall interactions
Fire safety
Flame retardants
Chemical reaction mechanism
Skeletal reduction

ABSTRACT

Organophosphorous compounds can act as chemical inhibitors for fire suppression and have recently received significant attention in the combustion community due to their potential to induce flame extinction through a radical recombination process. To optimize their use, a comprehensive understanding of the extinction dynamics is essential. In this study, mixtures of methane with dimethyl methylphosphonate (DMMP) are investigated in laminar conditions, with a specific focus on flame–wall interaction. The ultimate objective is obtaining a deeper insight into the flame quenching process, which is synergistically enhanced by heat transfer to the wall and the chemical retardant effect of DMMP. Detailed chemistry information is implemented by setting up an ad-hoc skeletal kinetic mechanism. This is developed and validated for flame configurations with increasing complexity, including freely propagating premixed flames, head-on-quenching flames, and side-wall quenching flames. The results indicate that the skeletal mechanism is able to reproduce available experimental data for flame speed and ignition delay time, as well as the main flame features and quenching characteristics in flame–wall interactions for an increasing level of DMMP. Simulations of a side-wall quenching burner, incorporating a secondary fuel injection through a porous insert at the wall, are carried out. Chemical analyses provide detailed insight into the role of flame retardant during the flame quenching process. The results show that the HOPO/PO_2 catalytic cycle is of major importance for the suppressant effect, further supported by the formation of CH_3PO_2 as an intermediate, increasing the formation of HOPO itself. Moreover, the CO mass fraction is observed to increase also because of the radical scavenging effect, inhibiting the conversion to CO_2 via CO + OH → CO_2 + H. Overall, this study advances the understanding of the chemical features of flame quenching in the presence of flame retardants containing implications for fire safety applications.

1. Introduction

In safety engineering, the chemical inhibition of combustion processes is essential for the prevention and suppression of fires [1]. To counteract fire spread and lengthen escape times, flame retardants (FRs) are used and, in some cases, integrated into materials such as polymers. Polymers with FRs are widely used for critical parts and components e.g., in the transportation sector, furniture, and electronic equipment. Flame retardants can contribute to the gas phase reactions with flame inhibition effects, but may also promote the char formation on the polymer surface, which reduces the release of volatiles and can act as a protective coating for the underlying unburned material [2]. In the past, flame-retardant research focused on identifying suitable chemicals that not only exhibit a high flame retardancy but are also non-toxic and climate-compatible. Phosphorous-containing compounds (PCCs) are among the most prominent groups of flame retardants, especially due to their comparably low toxicity and high efficiency [3]. Two commonly investigated PCCs are dimethyl methylphosphonate (DMMP, with a molecular formula $O=P(CH_3)(OCH_3)_2$) and trimethyl phosphate (TMP, $O=P(OCH_3)_3$).

Canonical experiments such as shock tube investigations [4], jet stirred reactor [5], counterflow [6] and premixed flames [7–9] provided insights into the inhibition mechanism and effectiveness of various PCCs. Sikes et al. [10] assessed the inhibition mechanism of DMMP, TMP, and diethyl methylphosphonate (DEMP) in spherically propagating hydrogen-air and methane–air flames. Bouvet et al. [11] investigated the effect of DMMP in co-flow diffusion flames, doping the fuel and the oxidizer stream. Their results indicated that the inhibition effectiveness of PCCs depends significantly on the flame type [11]. Furthermore, the authors observed a saturation of the inhibition effect for high concentrations of DMMP.

* Corresponding author.
E-mail address: alessandro.stagni@polimi.it (A. Stagni).

https://doi.org/10.1016/j.proci.2024.105529
Received 4 December 2023; Accepted 19 June 2024
Available online 25 July 2024

By leveraging such experimental datasets, detailed kinetic mechanisms for DMMP in hydrocarbon mixtures were developed [7,12], with several subsequent improvements and extensive validation [8,13,14]. Numerical simulations were mainly presented in one-dimensional laminar flames to analyze the inhibition effectiveness of PCCs [8,13,15]. From these chemical kinetics investigations, the high fire suppression capability of the PCCs can be attributed to their scavenging activity targeting radicals such as H, O, and OH [14].

During the onset and spread of fire, multi-physics thermo-chemical processes occur at the surface of a flammable compound in the vicinity of walls. In these configurations, near-wall flames are subject to heat transfer to the walls, depending on their thermal conditions, which affects the combustion chemistry. While flame–wall interaction (FWI) has been intensively studied both experimentally (e.g., [16,17]) and numerically, aiming at understanding the flame quenching process and the formation of pollutants (e.g., [18,19]), only a few works have explored the flame–wall interaction phenomenon in combination with a flame retardant for fire prevention.

Steinhausen et al. [20] recently investigated the retardant effect of PCC of flame–wall interaction of gaseous hydrocarbon fuels. Here, a combined experimental and numerical study investigated a vertical side-wall quenching (SWQ) flame including an active wall portion, consisting of a porous insert that supplies additional gaseous fuel. The SWQ configuration is adapted from the one studied in [19,21]. The active wall portion is located upstream of the quenching point, thus affecting the flame–wall interaction and flame extinction with a combined thermo-chemical process. Experimental data for pure methane (CH_4) supplied by the active wall was used to validate the numerical setup. Subsequently, the effect of seeding DMMP into the methane at the wall inlet was numerically investigated, varying the amount of DMMP.

In this study, still considering CH_4 as target fuel, the burner configuration from [20] is further investigated, focusing on the synergistic role of PCCs chemistry and heat transfer during quenching near the wall. To this end, a detailed kinetic framework is set up, which has been proven essential in previous works for accurately capturing both heat release rates and species formation [19,22]. Established core mechanisms for CH_4 and DMMP, previously validated in a wide range of operating conditions, are selected as building blocks of a comprehensive mechanism, which undergoes a preliminary skeletal reduction based on the SWQ operating conditions. A parametric study is performed, investigating the effect of varying amounts of DMMP on the quenching characteristics in the SWQ configuration. The combined role of flame retardant chemistry and heat losses to walls is studied by means of reaction flux analyses. Such a numerical study was performed by adopting GRI mech 3.0 [23], i.e. an established optimized mechanism describing CH_4 combustion, combined with the DMMP mechanism of Babushok et al. [14]. To the authors' knowledge, so far no previous study has been carried out on the role of flame retardants chemistry on SWQ starting from a detailed mechanism and leveraging the information contained in it. Therefore, building on this latest point, the objective of this work is threefold:

1. Develop and validate a skeletal kinetic mechanism able to accurately predict the flame suppression effect for various amounts of DMMP in FWI scenarios, with the right trade-off in terms of its accuracy and computing times of CFD simulations;
2. Investigate the impact of varying the amount of DMMP injected from an active wall on the thermochemical state near the quenching point;
3. Unravel the synergistic effect of chemical kinetics of PCCs and heat transfer to the wall on the flame quenching.

The results of this study are relevant to gain further insight into the inhibition mechanism of DMMP in close proximity to walls and its optimal application as a flame retardant compound.

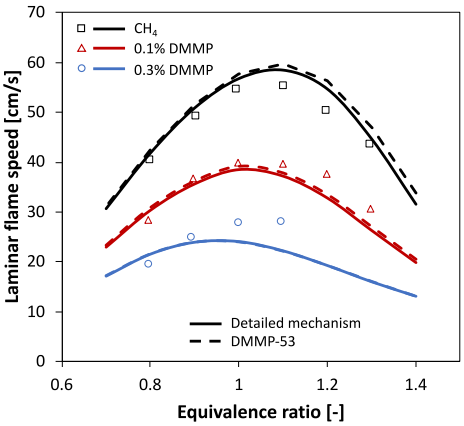

Fig. 1. Laminar flame speed of CH_4, with and without the addition of DMMP (0.1% and 0.3% mole fraction, respectively). T_u = 393 K. Experimental data [10] vs. modeling results, obtained with detailed and skeletal mechanism.

2. Kinetic modeling and reduction

The ultimate objective of this work is leveraging the information contained in detailed chemistry to investigate the dynamics of DMMP retardancy in flame–wall interaction with predictive features. In order to obtain predictive information in reasonable times, a unique workflow was set up, starting from the development of a comprehensive detailed mechanism, describing DMMP chemistry and related interactions with small hydrocarbons, then performing skeletal reduction on the whole mechanism.

The kinetic mechanism for CH_4 oxidation and related interaction with DMMP was set up by following a hierarchical and modular methodology. With regard to CH_4 modeling, the whole C_0-C_3 model was adopted from Bagheri et al. [24]. On the other hand, DMMP thermochemistry was incorporated by relying on the studies of Jayaweera et al. [13] and Korobeinichev et al. [8], who revisited the theoretical understanding of reactions involving small phosphorus-based species, fostering radical recombination and thus playing a role in flame suppression. Furthermore, they re-evaluated the thermodynamic properties of PO_xH_y species. The comprehensive mechanism developed through this approach included 162 species and 2399 reactions.

To integrate detailed kinetics into the SWQ simulations, a skeletal reduction procedure was applied to the mechanism. This was executed by using the approach outlined in [25], and implemented in the `DoctorSMOKE++` tool, coupling the Directed Relation Graph with Error Propagation (DRGEP) method [26] with Sensitivity Analysis [27], setting a maximum error threshold on ignition delay time equal to 10%. Reaction states were sampled by distributing 0D, constant-pressure homogeneous reactors uniformly across the defined operational space. This included atmospheric pressure, and a lean-to-rich composition range ($0.3 \leq \Phi \leq 2$). The final, reduced mechanism includes 53 species and 360 reactions. Detailed and reduced mechanisms are available in CHEMKIN format as Supplementary Material, along with thermodynamic and transport properties.

Prior to its application in SWQ simulations, the predictive capabilities of both mechanisms were evaluated by predicting ignition delay time and laminar flame speed of CH_4 with and without DMMP addition at near-atmospheric pressure, in conditions where experimental data are available in the literature. Fig. 1 shows the results related to laminar flame speed, compared with the data obtained by Sikes et al. [10] for variable additions of DMMP (with a maximum 0.3% amount, due to flame extinction afterwards), showcasing the effectiveness of both the starting mechanism as well as the reduced one. Similarly, in Fig. 2, a very good agreement can be appreciated for the ignition delay time, at different equivalence ratios (Φ), compared with the experimental

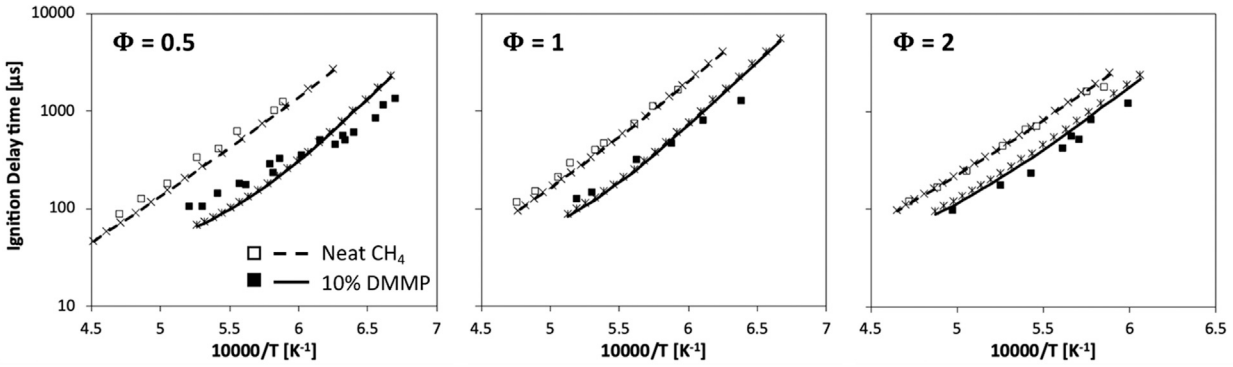

Fig. 2. Ignition delay time of CH_4/O_2 mixtures in a Shock tube (balance gas: 98% Ar mol/mol), with and without 10% DMMP, at variable Φ. Experimental data (squares) from [4]. Lines: detailed mechanism. Crosses: reduced mechanism.

results of Mathieu et al. [4]. Both mechanisms are able to predict the interestingly promoting effect of DMMP on CH_4, which although counterintuitive was noticed to the same extent in the experimental measurements.

3. Numerical configurations

3.1. Head-on quenching flame (HOQ)

In the head-on quenching (HOQ) configuration, a laminar freely-propagating premixed flame approaches a wall in the perpendicular direction, subsequently undergoing a quenching process due to heat losses. For the wall, typically a fixed temperature is prescribed. The physical flame characteristics, which occur during HOQ, can be transferred to other flame–wall interaction scenarios, making the one-dimensional flame configuration a well-suited canonical case for near-wall reacting flows. Numerical models for this configuration are well-established and readers are referred to Ref. [21] for further details.

3.2. Side-wall quenching flame (SWQ)

The burner configuration investigated in [20] is utilized in this work and is shown in Fig. 3. The burner is operated at ambient conditions (around 293.15 K, 1 atm) with laminar inflow. At the main inlet, a fully premixed stoichiometric methane–air flow is injected into the domain at a Reynolds number of $\approx$ 5900. A V-flame stabilization is achieved experimentally by employing a ceramic rod with a diameter of 1 mm. One flame branch interacts with a cold wall at a temperature stabilized (water-cooled) around 333 K and undergoes side wall quenching. To mimic an active wall (i.e., a wall participating in combustion processes), a porous media (sintered structure inlay) is inserted inside the vertical wall upstream of the quenching point, as illustrated in Fig. 3. The secondary wall inlet is positioned 30.5 mm downstream of the main nozzle and has a height of 5 mm. A constant volume flux of 2.0 L/h is injected through the porous media at around 373.15 K to prevent DMMP condensation [20]. Different amounts of DMMP are premixed with methane and injected into the domain through the porous wall inlet. A pure methane injection is also considered as the reference case, similar to [20], to facilitate the investigation of DMMP effects on the thermochemical state and flame characteristics.

Following previous numerical investigations of the SWQ burner [19–21], the current numerical setup consists of a two-dimensional planar subdomain of the quenching flame interacting with the cold wall. The domain has a length of 6 mm in the wall-normal direction and a height of 40 mm in the wall-parallel direction, as shown in Fig. 3. The computational mesh has a uniform spacing of 50 μm in all directions, resulting in 96000 cells in total. A grid sensitivity study (not shown for brevity) indicates that this resolution is sufficient to characterize the FWI in this configuration. A time step of 2 μs is employed that results in a maximum CFL number of 0.3. The main inflow is modeled using a parabolic velocity profile, while hot exhaust gases are injected through a 0.5 mm wide section [19,21]. Further details on the numerical setup of the SWQ configuration can be found in [20].

Finite-rate chemistry simulations are carried out by solving governing equations for the mass, momentum, species mass fractions, and enthalpy. Zero-gradient boundary conditions are applied for the enthalpy, species, and velocity at the top and right outlets. A Dirichlet boundary condition is employed for the pressure. A no-slip boundary condition for the velocity and a constant temperature of 333 K are applied at the passive portion of the vertical wall and a zero gradient boundary condition is employed for the species. At the wall inlet (WI), a zero gradient boundary condition for the pressure is used, while the velocity is assumed to be uniform over the inlet; a Robin boundary condition is applied for the species that accounts for both diffusive and convective fluxes

$$\dot{m}_{\mathrm{Wall}} Y_{k,\mathrm{in}} = \dot{m}_{\mathrm{Wall}} Y_k - \rho D_k^{\mathrm{mix}} \left(\frac{\partial Y_k}{\partial n_w} - \frac{Y_k}{\overline{W}} \frac{\partial \overline{W}}{\partial n_w} \right) + \rho V_w^{\mathrm{corr}} , \quad (1)$$

with $Y_{k,\mathrm{in}}$ the mass fraction of the species k in the injected wall mixture, Y_k the local mass fraction of species k, D_k^{mix} the mixture-averaged diffusion coefficient, and $\overline{W}$ the mean molecular weight. Gradients ($\partial/\partial n_w$) and vectors, such as the correction velocity V_w^{corr}, are projected in the wall-normal direction. Keeping constant volume flow through the wall inlet, the mass fraction of CH_4 in the mixture with DMMP is given as $Y_{\mathrm{CH_4,in}} = 1 - Y_{\mathrm{DMMP,in}}$.

The finite-rate chemistry simulations are performed using an in-house solver based on OpenFOAM (v2012), incorporating the DLBFoam library [28] for dynamic load balancing of the chemistry ODEs and Cantera [29] for the calculation of the species diffusion coefficients according to a mixture-averaged transport approach [30]. As shown in [20], the radiative heat transfer has a negligible effect on the results and it is therefore not accounted for.

4. Results and discussion

In this section, the mechanism assessment is firstly performed on a head-on-quenching (HOQ) flame configuration to confirm that the reduced mechanism captures the relevant physics during the flame quenching at the wall, with and without DMMP (Section 4.1). Subsequently, numerical simulations of the SWQ configuration featuring an active wall portion are carried out using the skeletal mechanism. The simulation results are analyzed (Section 4.2) and a reaction pathway analysis is performed to gain further insight into the chemical effect of the DMMP at the flame quenching (Section 4.3).

4.1. Mechanism assessment for 1D HOQ flames

In the HOQ configuration, the DMMP concentrations in the fresh gases are varied between zero, 1000 ppm, and 3000 ppm. The temper-

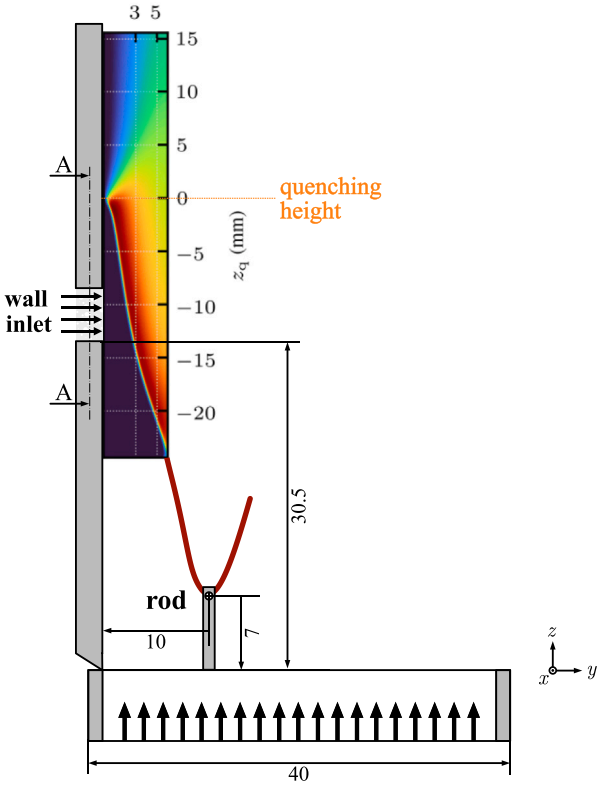

Fig. 3. Schematic representation of the SWQ burner and the numerical subdomain employed for simulation [20]. The dimensions are given in millimeters.

ature of the fresh gases and the wall is specified as 393 K (above the condensation temperature of DMMP). Fig. 4 shows the comparison of the wall heat flux versus time. For a convenient comparison, the wall heat flux profiles are aligned at the time of the peak value. As expected, the addition of the flame retardant significantly reduces the wall heat flux (peak and integral), even though the thermal load is transferred over a slightly longer time period when adding the flame retardant. From visual inspection, the results obtained with the detailed and the reduced mechanism show a close agreement. Deviations for the peak values remain below 2% for all considered cases.

Further investigating the predictions for key species, we examine the temporal evolution of the intermediates CH_2O and HOPO for the case with 3000 ppm DMMP, which is depicted in Fig. 5. The figure shows that these species exhibit a maximum inside of the flame front, which gets dissipated as the flame quenches at the wall. Again, the time axis is shifted such that the peak of the wall heat flux is located at $t = 0$ ms (marked by a horizontal dashed line). Overall, the species evolution predicted with both mechanisms shows only very minor deviations, which holds also true for major species and for cases with less DMMP (not shown). These results illustrate that the influence of flame retardants on HOQ of the premixed methane–air flame is accurately captured by the reduced mechanism, with a reduction of the computational time of about 80% compared to the detailed mechanism. Next, the novel mechanism is applied in simulations of the SWQ configuration.

4.2. SWQ flames with DMMP addition

In this section, the simulation results of the SWQ burner with increasing concentration of DMMP are discussed. The skeletal mechanism validated in the previous sections is employed. Following [17], the quenching height (z_q) is defined as the position of the maximum heat flux at the wall, while the quenching distance (y_q) is determined as the

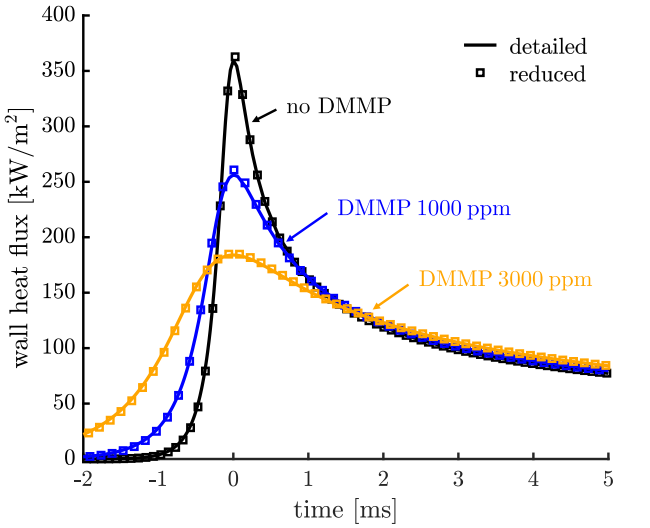

Fig. 4. Wall heat flux evaluated for lean premixed methane–air flames (T_0 = 393 K, p = 1 atm, ϕ = 0.8) undergoing HOQ with varying concentrations of DMMP (0/1000/3000 ppm) with the detailed and the reduced mechanism.

distance from the wall to the 1450 K temperature isoline at the specific quenching height.

Three mixture compositions are considered at the wall inflow with DMMP mass fraction $Y_{\mathrm{DMMP,in}}$ = 0, 0.1, and 0.3. It is noteworthy that the quantity of DMMP injected through the wall inflow mixture is much larger than the amount of DMMP present in the composition boundary layer downstream of the porous matrix (almost one order of magnitude, as shown in the following). This is due to the very low inflow velocity, i.e., $u_{WI}/u_{bulk} < 0.3\%$). The amount of DMMP is selected based on previous experimental studies on canonical premixed flames [10], indicating flame extinction for larger DMMP content.

The comparison with [20] shows very a good agreement for $Y_{\mathrm{DMMP,in}} = 0.3$ with quenching distance y_q equal to 0.484 mm compared to 0.465 mm. Fig. 6 illustrates the contour plots of the temperature, CO and HOPO mass fractions, two intermediate compounds formed during methane and DMMP oxidation, and the local heat release rate (HRR) in the vicinity of the quenching point (QP). The coordinate system is defined relative to the quenching height of the case with $Y_{\mathrm{DMMP,in}} = 0$. The temperature and CO contour plot include the 1450 K temperature isoline and the quenching point. In the HOPO and HRR contours, the isolines of the DMMP mass fraction are additionally presented. Both species are produced in the reaction zone (HRR $> 2 \cdot 10^8$ W/m^3), where DMMP and CH_4 are consumed, reaching their peaks close to the quenching point. For the pure methane wall injection ($Y_{\mathrm{DMMP,in}} = 0$), the maximum CO mass fraction is concentrated along the reaction zone and decreases rapidly downstream of the QP. In contrast, with DMMP addition, elevated values of CO mass fraction are observed also largely downstream of the QP, in the near wall region. HOPO is formed in the region where the DMMP (indicated by mass fraction isolines) interacts with the reaction zone, and akin to CO contour, in the same region downstream of the QP, within the near-wall region. This indicates the effect of flame retardants in chemically quenching the flame, resulting in an increase of incomplete combustion products like CO. This observation aligns with the findings of pyrolysis experiments of polymers containing PCC flame retardants [31]. Furthermore, the formation of CO in FWI is of great importance due to its toxicity and relevance for fire protection. To gain deeper understanding of the chemical effects of the DMMP in the quenching zone, the mixture composition is extracted along three horizontal planes: at QP and both upstream (z_q = −3 mm) and downstream (z_q=2 mm) of it. The key chemical reactions are identified and analyzed in the following section.

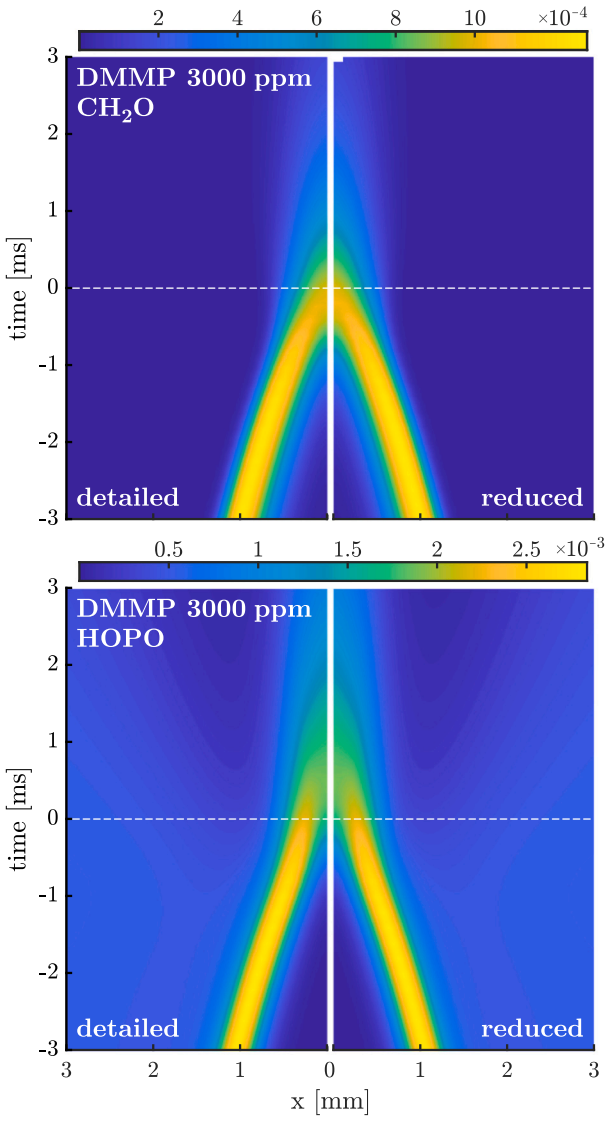

Fig. 5. CH_2O and HOPO evolution during HOQ of a premixed CH_4-air flame (T_0 = 393 K, p = 1 atm, ϕ = 0.8) with DMMP simulated with detailed and reduced mechanisms.

4.3. Role of DMMP chemistry in SWQ

As discussed by Jayaweera et al. [13] and Korobeinichev et al. [8], the suppressant effect of PCCs must be attributed to the net recombination of H and OH radicals, having phosphorus dioxide (PO_2), HOPO and $HOPO_2$ as radical scavengers. Such behavior is confirmed in the flux analysis shown in Fig. 7, performed at the quenching point with $Y_{DMMP,in}$ = 0.3. Here, oxygen was used as reference atom as common to all of the P-containing species involved. For the sake of clarity, the starting species is $PO(OH)_3$, which is formed in the early stages of DMMP decomposition, as also noticed by Jayaweera et al. [13] in premixed conditions. This later decomposes into the smaller phosphorous compounds, as confirmed by the mole fraction profiles shown in Fig. 8: the residual fuel peaks at the wall, while progressively decomposing into smaller species when getting farther from the wall.

The core of the cycle resulting in flame suppression is represented by the termination of H and OH into H_2O because of the gas-phase catalytic cycles between PO_2 and HOPO, occurring via PO_2+H+M → HOPO+M and HOPO+OH → PO_2+H_2O. Such effect is reinforced by the parallel loop involving C-P interaction through the formation of CH_3PO_2, with methyl radical as intermediate product: PO_2+CH_3 → CH_3PO_2 and CH_3PO_2+H → HOPO+CH_3. In correspondence with the quenching point, such a path gives a contribution to HOPO formation, equal to about one-third of the main route, which cannot be neglected anyway. On the other hand, the PO_2/$HOPO_2$ cycle (PO_2+OH+M → $HOPO_2$+M and $HOPO_2$+H → PO_2+H_2O) plays a negligible role, which is expected due to rich conditions. Although $HOPO_2$ is significantly formed via decomposition of $PO(OH)_3$, its termination reaction is only 1/5 of the major path via HOPO. To this regard, Fig. 9 provides the variation of reaction rates involving HOPO and $HOPO_2$ termination along the horizontal line passing through the quenching point as well as immediately upstream (z_q = −3 mm) and downstream (z_q = 2 mm).

In addition to the difference by an order of magnitude between the two reaction rates, the substantial modification of the OH profile due to the wall injection can be seen, with maximum deviations close to z_q. As a consequence, a double peak can be observed for both reaction rates: the first one is due to the high concentration of HOPO and $HOPO_2$ as intermediate species close to the wall, while the second one is the result of the increasing OH concentration farther from the wall, where it tends to converge to the value predicted in absence of DMMP. Expectably, this results in an increase of the unburned CO, whose peak reaction rate related to its conversion to CO_2 (CO+OH → CO_2+H) drops by a factor ∼4 at the quenching point. Therefore, the carbon selectivity is consequently affected in favor of CO downstream of the quenching point, as shown in Fig. 10.

5. Conclusions

Research efforts on flame–wall interaction were often focused on improving engine performance and reducing pollutant formation. While FWI configurations are also key in fire safety, aiming at flame suppression, only few numerical studies have been conducted in this context, specifically addressing FR effects on flames spreading over active walls.

In this study, the synergistic effects of phosphor-based flame retardants and wall heat transfer have been hierarchically investigated, analyzing FWI configurations with increasing complexity. To accommodate detailed chemistry into the CFD solver, a skeletal reduction methodology was applied starting from established mechanism blocks for CH_4 and phosphorus-based compounds. The reduction allows to reduce the complete mechanism (162 species and 2399 reactions) to 53 species and 360 reactions. The reduced mechanism shows only minor deviations from the detailed mechanism for key flame features and quenching characteristics, such as the laminar flame speed, wall heat flux, and flame structure (with and without FRs).

The novel mechanism has been used to investigate a SWQ burner configuration. The burner features an active portion of the wall that introduces additional fuel, or fuel mixed with flame retardants. This interacts with a premixed stoichiometric CH_4/air flame in the vicinity of a cold wall. The analysis reveals that the addition of flame retardants increases the quenching distance, moving the quenching point away from the wall. From a chemical perspective, DMMP enhances incomplete combustion by scavenging OH molecules. Thereby, CO increases significantly downstream of the QP due to the consequent drop in the rate of CO+OH → CO_2+H. This is of significant relevance in fire safety due to CO toxicity. Finally, the present work shows that skeletal reduction workflows can be safely adopted also for fire safety applications, for efficient and accurate numerical simulations under the influence of flame retardants.

Novelty and Significance Statement

This study presents a systematic investigation of the synergistic effect of phosphorous-containing compounds (PCC) and heat transfer in near-wall flame quenching. A crucial novelty is the derivation of a skeletal mechanism, which includes hydrocarbons and PCC kinetics. The mechanism is hierarchically validated using experimental datasets

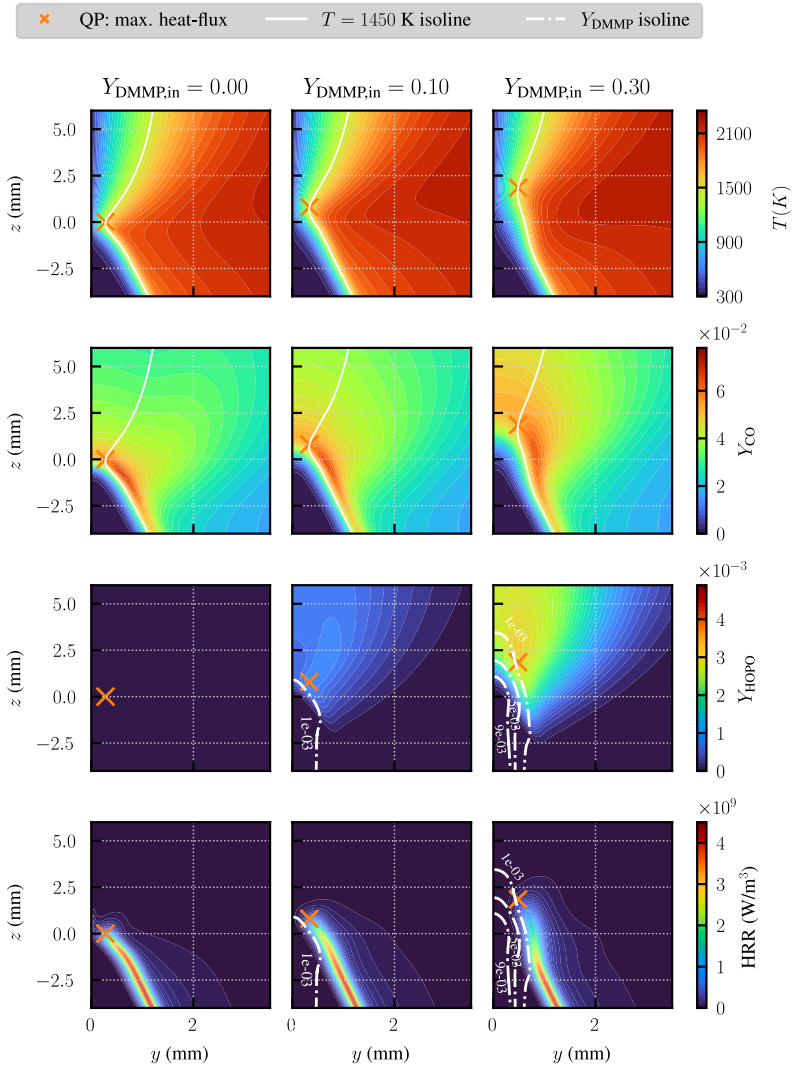

Fig. 6. Contours of temperature (top), CO and HOPO mass fraction (center), and local heat release rate (HRR) (bottom) for different amounts of DMMP in the wall inlet mixture. The first two rows display the 1450 K temperature isoline along with the location of the quenching point, while third and forth rows show isolines of the DMMP mass fraction as dashed–dotted lines.

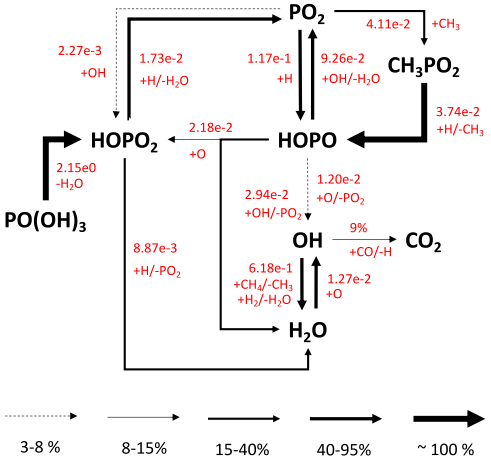

Fig. 7. Oxygen flux analysis starting from PO_2, performed at the quenching point for the case with $Y_{DMMP,in}$ = 0.3. The arrow thickness is relative to the single molecule.

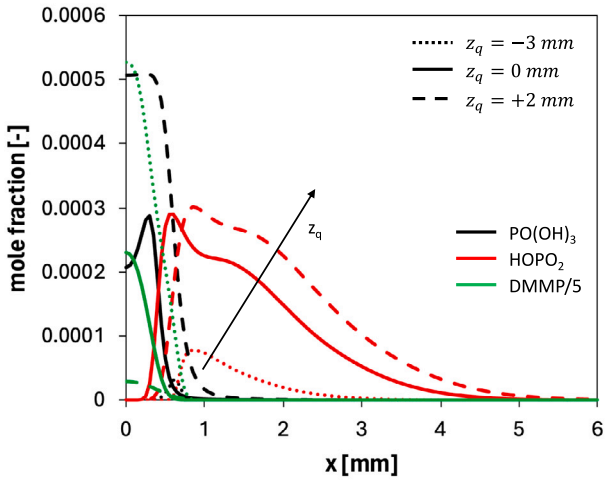

Fig. 8. Mole fractions of $PO(OH)_3$ and $HOPO_2$, respectively, at three different heights, as obtained in the case with $Y_{DMMP,in}$ = 0.3.

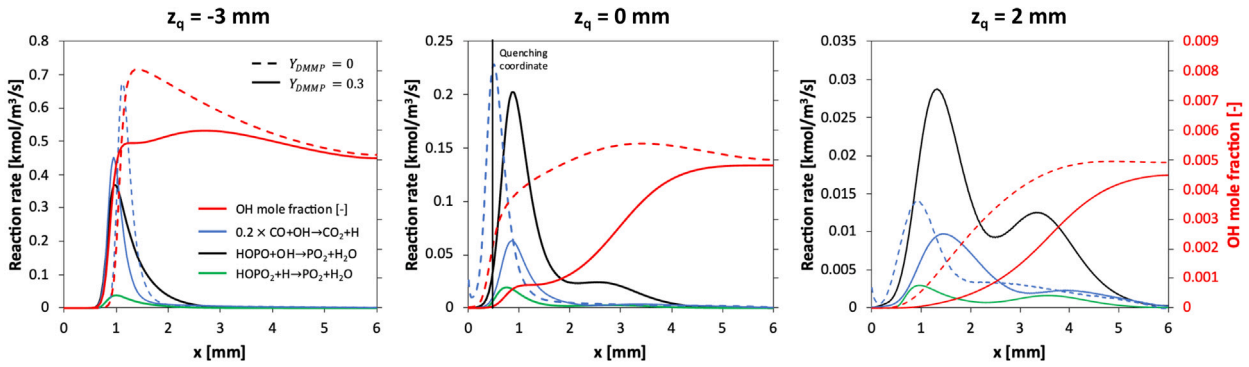

Fig. 9. Reaction rates of HOPO/$HOPO_2$ termination and CO conversion to CO_2, and OH mole fractions at three different heights, as obtained in the pure case and with $Y_{DMMP,in} = 0.3$.

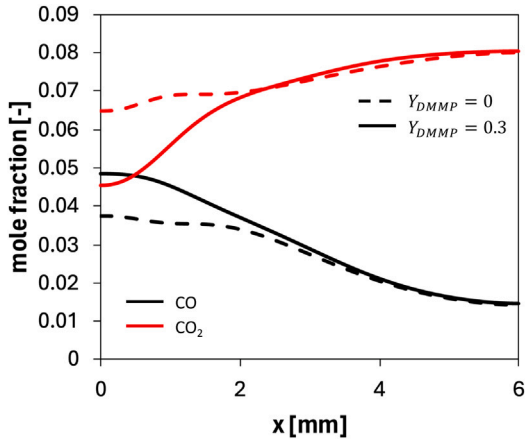

Fig. 10. Mole fractions of CO and CO_2 downstream of the quenching point with and without DMMP addition, at $z_q = 2$ mm.

and detailed kinetic simulations. The newly developed mechanism (53 species and 360 reactions) is key for enabling efficient detailed numerical simulations in fire safety applications, reducing the computational time. Further, numerical investigations of a side-wall quenching burner with an active wall insert confirm experimental observations: PCCs inhibit chemical reactions by scavenging OH, leading to incomplete combustion and an increased CO mass fraction at the quenching point and in the near wall region.

CRediT authorship contribution statement

Federica Ferraro: Conceptualization, Investigation, Data curation, Writing – original draft, Funding acquisition. **Alessandro Stagni:** Conceptualization, Investigation, Data curation, Writing – original draft. **Arne Scholtissek:** Conceptualization, Investigation, Data curation, Writing – original draft, Funding acquisition.

Declaration of competing interest

The authors declare that they have no known competing financial interests or personal relationships that could have appeared to influence the work reported in this paper.

Acknowledgments

This work has been funded by the Deutsche Forschungsgemeinschaft (DFG, German Research Foundation) – Project Number 237267381 – TRR 150. We thank Prof. B. Schartel for the fruitful discussions on flame retardants. We further thank R. Strickling for his support in conducting the simulations.

Appendix A. Supplementary data

Supplementary material related to this article can be found online at https://doi.org/10.1016/j.proci.2024.105529.

References

[1] A.R. Masri, Chemical inhibition of nonpremixed flames of hydrocarbon fuels with CF3Br, Combust. Sci. Technol. 96 (1994) 189–212.
[2] E. Schmitt, Phosphorus-based flame retardants for thermoplastics, Plast. Addit. Compd. 9 (2007) 26–30.
[3] L. Wang, Y. Jiang, R. Qiu, Experimental study of combustion inhibition by trimethyl phosphate in turbulent premixed methane/air flames using OH-PLIF, Fuel 294 (2021) 120324.
[4] O. Mathieu, W.D. Kulatilaka, E.L. Petersen, Experimental and modeling study on the effects of dimethyl methylphosphonate (DMMP) addition on H_2, CH_4, and C_2H_4 ignition, Combust. Flame 191 (2018) 320–334.
[5] Y. Jing, J. Cui, B. Liu, Q. Zhu, Q. Xu, Z. Hu, F. Fu, L. Xing, Z. Wang, Pyrolysis and kinetic study of dimethyl methylphosphonate (DMMP) by synchrotron photoionization mass spectrometry, Combust. Flame 255 (2023) 112919.
[6] M.A. MacDonald, T.M. Jayaweera, E.M. Fisher, F.C. Gouldin, Inhibition of nonpremixed flames by phosphorus-containing compounds, Combust. Flame 116 (1999) 166–176.
[7] O.P. Korobeinichev, V.M. Shvartsberg, T.A. Bol'shova, A.G. Shmakov, D.A. Knyaz'kov, Inhibition of methane-oxygen flames by organophosphorus compounds, Combust. Explor. Shock Waves 38 (2002) 127–133.
[8] O.P. Korobeinichev, V.M. Shvartsberg, A.G. Shmakov, T.A. Bolshova, T.M. Jayaweera, C.F. Melius, W.J. Pitz, C.K. Westbrook, H. Curran, Flame inhibition by phosphorus-containing compounds in lean and rich propane flames, Proc. Combust. Inst. 30 (2005) 2353–2360.
[9] I.V. Rybitskaya, A.G. Shmakov, V.M. Shvartsberg, O.P. Korobeinichev, Effect of the equivalence ratio on the effectiveness of inhibition of laminar premixed hydrogen-air and hydrocarbon-air flames by trimethylphosphate, Combust. Explor. Shock Waves 44 (2008) 133–140.
[10] T. Sikes, O. Mathieu, W.D. Kulatilaka, M.S. Mannan, E.L. Petersen, Laminar flame speeds of DEMP, DMMP, and TEP added to H_2- and CH_4-air mixtures, Proc. Combust. Inst. 37 (2019) 3775–3781.
[11] N. Bouvet, G. Linteris, V. Babushok, F. Takahashi, V. Katta, R. Krämer, Experimental and numerical investigation of the gas-phase effectiveness of phosphorus compounds, Fire Mater. 40 (2016) 683–696.
[12] P.A. Glaude, H.J. Curran, W.J. Pitz, C.K. Westbrook, Kinetic study of the combustion of organophosphorus compounds, Proc. Combust. Inst. 28 (2000) 1749–1756.
[13] T.M. Jayaweera, C.F. Melius, W.J. Pitz, C.K. Westbrook, O.P. Korobeinichev, V.M. Shvartsberg, A.G. Shmakov, I.V. Rybitskaya, H.J. Curran, Flame inhibition by phosphorus-containing compounds over a range of equivalence ratios, Combust. Flame 140 (2005) 103–115.
[14] V.I. Babushok, G.T. Linteris, V.R. Katta, F. Takahashi, Influence of hydrocarbon moiety of DMMP on flame propagation in lean mixtures, Combust. Flame 171 (2016) 168–172.
[15] F. Takahashi, V. Katta, G. Linteris, V. Babushok, Numerical study of gas-phase interactions of phosphorus-containing compounds with co-flow diffusion flames, Proc. Combust. Inst. 37 (2019) 4145–4153.
[16] A. Dreizler, B. Böhm, Advanced laser diagnostics for an improved understanding of premixed flame-wall interactions, Proc. Combust. Inst. 35 (2015) 37–64.
[17] H. Kosaka, F. Zentgraf, A. Scholtissek, L. Bischoff, T. Häber, R. Suntz, B. Albert, C. Hasse, A. Dreizler, Wall heat fluxes and CO formation/oxidation during laminar and turbulent side-wall quenching of methane and DME flames, Int. J. Heat Fluid Flow 70 (2018) 181–192.

[18] A. Gruber, R. Sankaran, E.R. Hawkes, J.H. Chen, Turbulent flame–wall interaction: a direct numerical simulation study, J. Fluid Mech. 658 (2010) 5–32.
[19] M. Steinhausen, Y. Luo, S. Popp, C. Strassacker, T. Zirwes, H. Kosaka, F. Zentgraf, U. Maas, A. Sadiki, A. Dreizler, C. Hasse, Numerical investigation of local heat-release rates and thermo-chemical states in side-wall quenching of laminar methane and dimethyl ether flames, Flow Turbul. Combust. 106 (2021) 681–700.
[20] M. Steinhausen, F. Ferraro, M. Schneider, F. Zentgraf, M. Greifenstein, A. Dreizler, C. Hasse, A. Scholtissek, Effect of flame retardants on side-wall quenching of partially premixed laminar flames, Proc. Combust. Inst. 39 (2023) 3745–3754.
[21] S. Ganter, A. Heinrich, T. Meier, G. Kuenne, C. Jainski, M.C. Rißmann, A. Dreizler, J. Janicka, Numerical analysis of laminar methane–air side-wall-quenching, Combust. Flame 186 (2017) 299–310.
[22] A. Stagni, Y. Luo, M. Steinhausen, A. Dreizler, C. Hasse, Chemistry effects in the wall quenching of laminar premixed DME flames, Combust. Flame 232 (2021) 111529.
[23] G.P. Smith, D.M. Golden, M. Frenklach, N.W. Moriarty, B. Eiteneer, M. Goldenberg, C.T. Bowman, R.K. Hanson, S. Song, W.C. Gardiner, V.V. Lissianski, Z. Qin, GRI-mech 3.0, 1999, http://www.me.berkeley.edu/gri_mech/. (Accessed 26 May 2024).
[24] G. Bagheri, E. Ranzi, M. Pelucchi, A. Parente, A. Frassoldati, T. Faravelli, Comprehensive kinetic study of combustion technologies for low environmental impact: MILD and OXY-fuel combustion of methane, Combust. Flame 212 (2020) 142–155.
[25] A. Stagni, A. Frassoldati, A. Cuoci, T. Faravelli, E. Ranzi, Skeletal mechanism reduction through species-targeted sensitivity analysis, Combust. Flame 163 (2016) 382–393.
[26] P. Pepiot-Desjardins, H. Pitsch, An efficient error-propagation-based reduction method for large chemical kinetic mechanisms, Combust. Flame 154 (1–2) (2008) 67–81.
[27] K.E. Niemeyer, C.-J. Sung, M.P. Raju, Skeletal mechanism generation for surrogate fuels using directed relation graph with error propagation and sensitivity analysis, Combust. Flame 157 (9) (2010) 1760–1770.
[28] B. Tekgül, P. Peltonen, H. Kahila, O. Kaario, V. Vuorinen, DLBFoam: An open-source dynamic load balancing model for fast reacting flow simulations in OpenFOAM, Comput. Phys. Comm. 267 (2021) 108073.
[29] D.G. Goodwin, H.K. Moffat, I. Schoegl, R.L. Speth, B.W. Weber, Cantera: An object-oriented software toolkit for chemical kinetics, thermodynamics, and transport processes, 2023, http://dx.doi.org/10.5281/zenodo.8137090, https://www.cantera.org, version 3.0.0.
[30] T.P. Coffee, J.M. Heimerl, Transport algorithms for premixed, laminar steady state flames, Combust. Flame 43 (1981) 273–289.
[31] U. Braun, A. Balabanovich, B. Schartel, U. Knoll, J. Artner, M. Ciesielski, M. Döring, R. Perez, J. Sandler, V. Altstädt, T. Hoffmann, D. Pospiech, Influence of the oxidation state of phosphorus on the decomposition and fire behaviour of flame-retarded epoxy resin composites, Polymer 47 (2006) 8495–8508.